

***In situ* carbon coating for enhanced chemical stability of copper nanowires**

Xiaolan Tong, Hao Hu, Xingzhong Zhao, and Qidong Tai

Cite this article as:

Xiaolan Tong, Hao Hu, Xingzhong Zhao, and Qidong Tai, *In situ* carbon coating for enhanced chemical stability of copper nanowires, *Int. J. Miner. Metall. Mater.*, 29(2022), No. 3, pp. 557-562. <https://doi.org/10.1007/s12613-021-2343-x>

View the article online at [SpringerLink](#) or [IJMMM Webpage](#).

Articles you may be interested in

Oksana Velgosova, Elena ižmárová, Jaroslav Málek, and Jana Kavuliova, [Effect of storage conditions on long-term stability of Ag nanoparticles formed via green synthesis](#), *Int. J. Miner. Metall. Mater.*, 24(2017), No. 10, pp. 1177-1182. <https://doi.org/10.1007/s12613-017-1508-0>

Zhi-li Li, Feng Rao, Shao-xian Song, Yan-mei Li, and Wen-biao Liu, [Slime coating of kaolinite on chalcopyrite in saline water flotation](#), *Int. J. Miner. Metall. Mater.*, 25(2018), No. 5, pp. 481-488. <https://doi.org/10.1007/s12613-018-1594-7>

Hong Qin, Xue-yi Guo, Qing-hua Tian, and Lei Zhang, [Recovery of gold from refractory gold ores: Effect of pyrite on the stability of the thiourea leaching system](#), *Int. J. Miner. Metall. Mater.*, 28(2021), No. 6, pp. 956-964. <https://doi.org/10.1007/s12613-020-2142-9>

Ping-ping Wang, Guo-qin Chen, Wen-jun Li, Hui Li, Bo-yu Ju, Murid Hussain, Wen-shu Yang, and Gao-hui Wu, [Microstructural evolution and thermal conductivity of diamond/Al composites during thermal cycling](#), *Int. J. Miner. Metall. Mater.*, 28(2021), No. 11, pp. 1821-1827. <https://doi.org/10.1007/s12613-020-2114-0>

Pian Zhang, Yun-hao Wu, Hao-ran Sun, Jia-qi Zhao, Zhi-ming Cheng, and Xiao-hong Kang, [MnO₂/carbon nanocomposite based on silkworm excrement for high-performance supercapacitors](#), *Int. J. Miner. Metall. Mater.*, 28(2021), No. 10, pp. 1735-1744. <https://doi.org/10.1007/s12613-021-2272-8>

Huan-yu Zhang, Rui Li, Wen-wu Liu, Mei Zhang, and Min Guo, [Research progress in lead-less or lead-free three-dimensional perovskite absorber materials for solar cells](#), *Int. J. Miner. Metall. Mater.*, 26(2019), No. 4, pp. 387-403. <https://doi.org/10.1007/s12613-019-1748-2>



IJMMM WeChat



QQ author group

In situ carbon coating for enhanced chemical stability of copper nanowires

Xiaolan Tong¹⁾, Hao Hu²⁾, Xingzhong Zhao^{1),✉}, and Qidong Tai^{2),✉}

1) School of Physics and Technology, Wuhan University, Wuhan 430072, China

2) Institute of Technological Sciences, Wuhan University, Wuhan 430072, China

(Received: 24 April 2021; revised: 18 August 2021; accepted: 19 August 2021)

Abstract: Copper nanowires (CuNWs) are promising electrode materials, especially for used in flexible and transparent electrodes, due to their advantages of earth-abundant, low-cost, high conductivity and flexibility. However, the poor stability of CuNWs against oxidation and chemical corrosion seriously hinders their practical applications. Herein, we propose a facile strategy to improve the chemical stability of CuNWs by *in situ* coating of carbon protective layer on top of them through hydrothermal carbonization method. The influential factors on the growth of carbon film including the concentration of the glucose precursor (carbon source), hydrothermal temperature, and hydrothermal time are systematically studied. By tailoring these factors, carbon layers with thickness of 3–8 nm can be uniformly grown on CuNWs with appropriate glucose concentration around 80 mg·mL⁻¹, hydrothermal temperature of 160–170°C, and hydrothermal time of 1–3 h. The as-prepared carbon-coated CuNWs show excellent resistance against corrosion and oxidation, and are of great potential to use broadly in various optoelectronic devices.

Keywords: electrode material; copper nanowire; *in situ* carbon coating; stability

1. Introduction

Metal nanowires such as silver nanowires (AgNWs) and copper nanowires (CuNWs) with advantages of low cost, high flexibility, and good conductivity, are considered to be promising electrode materials, especially for transparent conductive electrode applications [1–2]. Compared to AgNWs, which have been widely used in various optoelectronic devices (e.g. sensors, organic light-emitting diodes, and solar cells) [3–6], comparable film transparency and conductivity can be achieved with CuNWs and copper is more advantageous in terms of material cost [7–14]. However, less attention has been paid to CuNWs, one possible reason could be that copper is less stable than silver, and CuNWs can be easily oxidized in ambient air, resulting in significant drop of the film conductivity [15–20].

The stability of CuNWs films against oxidation can be improved through protective coatings, for example, using aluminum (Al) doped ZnO (AZO), AZO/Al₂O₃ [18,20], and electroless nickel (Ni) as physical barriers [21]. However, the film conductivity and transparency are typically compromised in these cases, due to the increased surface roughness. It is also reported that highly conductive CuNWs film with enhanced oxidation resistance could be obtained by embedding the CuNWs network into pre-coated poly(3,4-ethylenedioxythiophene):poly(styrenesulfonate) (PEDOT:PSS) film [17], but the long-term stability of such composite film needs to be further verified, as the environmental stability of PE-

DOT:PSS is poor. Recently, CuNWs/graphene and CuNWs/reduced graphene oxide (rGO) core-shell nanowires have been proposed for preparing high performance transparent conducting electrodes with excellent stability, transparency, and conductivity [15–16,19]. In the former case, the graphene layer was deposited via plasma enhanced chemical vapor deposition method at temperature over 500°C, which is energy consuming and thus unfavorable for low-cost, large-scale production. In the latter case, though mild preparation conditions were used, the CuNWs/rGO core-shell nanowires had to be prepared in a complicated way, including the synthesis of GO, the coating of GO on CuNWs, and the thermal reduction of GO to rGO, which is disadvantageous for scalable production either. Therefore, it is meaningful to develop new facile and cost-effective methods that can be used to prepare stable core-shell structured CuNWs for high-performance transparent electrode applications.

Hydrothermal carbonization is a cheap and sustainable way to generate various carbon materials [22], which has been widely used to prepare carbon-coated nanoparticles (including metals) for achieving enhanced stability against oxidation and degradation [23–26]. It is therefore possible to produce carbon-coated metal nanowires through this method. Herein, we report the synthesis of carbon-coated CuNWs (CuNWs@C) using hydrothermal carbonization method with glucose precursor, and the influences of precursor concentration, hydrothermal temperature, and hydrothermal time on the growth of the carbon layer were systematically studied.

✉ Corresponding authors: Xingzhong Zhao E-mail: xzzhao@whu.edu.cn; Qidong Tai E-mail: qdtai@whu.edu.cn

Under appropriate condition, carbon layers with thickness around 3–8 nm could be uniformly coated on the surface of CuNWs. The coating of thin carbon film showed negligible influence on the conductivity and transmittance of the CuNWs, while significantly improved their stability against oxidation and chemical corrosion. The resulting CuNWs@C with high robustness are expected to be applied extensively in optoelectronic devices.

2. Experimental

2.1. Synthesis of CuNWs

50 mg $\text{CuCl}_2 \cdot 2\text{H}_2\text{O}$, 150 mg glucose, and 400 mg hexadecylamine were dissolved in 20 mL deionized (D. I.) water in a 25 mL vial. After stirred at room temperature for overnight, the mixture was heated at 100°C for 6 h [10]. Then the suspension was centrifuged and rinsed with hexane/isopropyl alcohol (IPA) for 3 times. Finally, the CuNWs were dispersed in 3 mL IPA. All of the chemicals were purchased from Sinopharm, China, and used without further purification.

2.2. Synthesis of CuNWs@C

0.5–3 g glucose was added into a mixed solution of 5 mL D. I. water and 10 mL IPA, to which the as-prepared CuNWs suspension in IPA (3 mL) was added. The mixed suspension was transferred into a 50 mL autoclave and heated at $160\text{--}200^\circ\text{C}$ for 1–5 h, followed by centrifuged and rinsed with the mixture of D. I. water and IPA for 2 times. Then the resulted CuNWs@C were dispersed in 3 mL IPA.

2.3. Preparation of CuNW and CuNW@C-based thin films

The as-prepared nanowire suspension in IPA was first diluted and then filtered through a cellulose acetate membrane. After that, the membrane with captured nanowires was transferred onto glass substrate by applying pressure on the backside of the membrane. Finally, the cellulose membrane was removed by dipping the substrate in acetone, followed by washing of the CuNW film with acetic acid or annealing of the CuNW@C film at 200°C in glovebox for 5 min to improve film conductivity.

2.4. Preparation of dye-sensitized solar cells (DSSCs)

The dye-sensitized TiO_2 photoanode, I^-/I_3^- electrolyte, and the polyaniline (PANI) nanoparticles were prepared ac-

ording to the procedures previously reported by our group [27–28]. The mixed solution of PANI and PEDOT:PSS was prepared by direct dispersing PANI nanoparticle in the commercial PEDOT:PSS solution (PH 1000, Clevios) at $2 \text{ mg} \cdot \text{mL}^{-1}$. The counter electrodes (CEs) were prepared by spin-coating of the mixed solution on CuNWs and CuNWs@C substrates and annealed at 130°C for 20 min. The DSSCs were assembled in a sandwich structure with electrolyte between the photoanodes and CEs.

2.5. Characterizations

The morphology of the nanowire was observed by scanning electron microscope (SEM; SU8010, Hitachi, Japan) and transmission electron microscope (TEM; JEF 2010 FEF, JEOL, Japan). The TEM sample was prepared by directly dropping of the diluted nanowire solution in IPA on Cu grid. The X-ray diffraction (XRD) was characterized using PANalytical X'Pert diffractometer. The sheet resistance of the nanowire-based film was measured using four-point probe method (RTS-4, Guangzhou 4-probe Tech Co., Ltd., China). The transmittance of the nanowire film was obtained with UV-Vis spectrometer (Lambda 650, Perkin-Elmer, USA). The photovoltaic performance of the DSSC was measured under air mass (AM) 1.5, $100 \text{ mW} \cdot \text{cm}^{-2}$ simulated illumination with an active device area of 0.25 cm^2 .

3. Results and discussion

Fig. 1 shows the schematic illustration of the method used for the preparation of CuNWs and CuNWs@C. The CuNWs were synthesized by the reduction of copper chloride (CuCl_2) by glucose with the presence of hexadecylamine (HDA) as capping agent, according to a one-pot procedure reported in the literature [10]. As can be seen in Fig. 2, the as-synthesized CuNWs with an average diameter around 50 nm, were up to tens of micrometers long, and could be well dispersed in IPA.

It has been shown in previous study that the glucose would suffer aromatization and carbonization under hydrothermal condition at temperatures over 160°C [23], which offers an ideal strategy for the *in situ* formation of carbon protective layer on CuNWs, if they are autoclaved together with glucose. To ensure the uniform growth of the carbon layer, the influences of the amount of glucose, the autoclave temperature and time were systematically studied. The total volume of the mixed solution used for hydrothermal process was fixed at 18

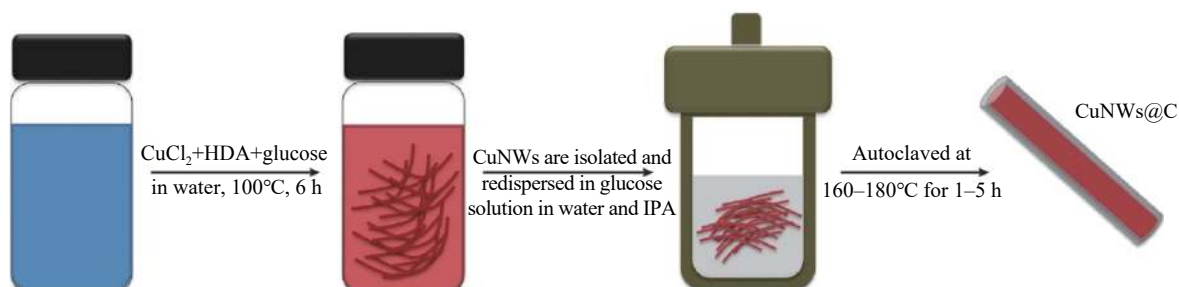


Fig. 1. Schematic illustration of the synthesis of copper nanowires (CuNWs) and carbon coated copper nanowires (CuNWs@C).

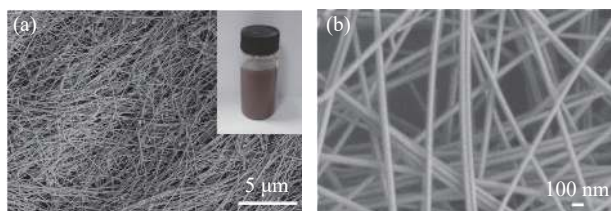


Fig. 2. SEM images of the as-synthesized CuNWs: (a) low magnification image; (b) high magnification image. The inset shows the dispersion of CuNWs in IPA.

mL (5 mL H₂O and 13 mL IPA), corresponding to a 36% filling of the 50 mL autoclave (the details were described in the experimental section).

In case of studying the influence of the concentration of the glucose, the autoclave temperature and time were fixed at 160°C and 3 h, respectively. It can be clearly seen from the TEM images in Fig. 3(a)–(c), the growth of carbon layer is directly related to the amount of glucose used. When a small amount of glucose was used (0.5 g, 27.8 mg·mL⁻¹), there was no uniform carbon layer formed. By contrast, smooth carbon layer with uniform thickness of ~8 nm was grown with higher amount of glucose (1.5 g, 83.4 mg·mL⁻¹). However, too much glucose (3 g, 116.8 mg·mL⁻¹) was found to result in

thick and rough carbon shell, which is possibly due to the over growth of the carbon layer caused by the increased growth rate at high concentration of glucose precursor.

Then, with fixed autoclave temperature of 160°C and an appropriate amount of glucose (1.5 g, 83.4 mg·mL⁻¹), the influence of autoclave time was investigated. As displayed in Fig. 3(d)–(f), a short autoclave time of 1 h was found enough to grow continuous carbon film on CuNW, but the film thickness was only 2–3 nm. Thicker carbon layer (~7 nm) was uniformly formed with longer autoclave time of 2 h, which was comparable to the result obtained at 3 h autoclave time (Fig. 3(b)). Similar to the influence of excessive glucose, prolonged autoclave time of 5 h also led to thicker carbon layer with rougher surface morphology. In this case, the non-uniform film growth could be ascribed to the heterogeneous surface reaction due to the exhaustion of the glucose precursor.

Finally, based on fixed amount of glucose (1.5 g, 83.4 mg·mL⁻¹) and autoclave time (2 h), the influences of higher autoclave temperatures of 170, 180, and 200°C were investigated. As shown in Fig. 3(g)–(i), the carbon layer grown at 170°C was identical to the case at 160°C. It seems that 180°C is a critical point for the growth of carbon film. At this tem-

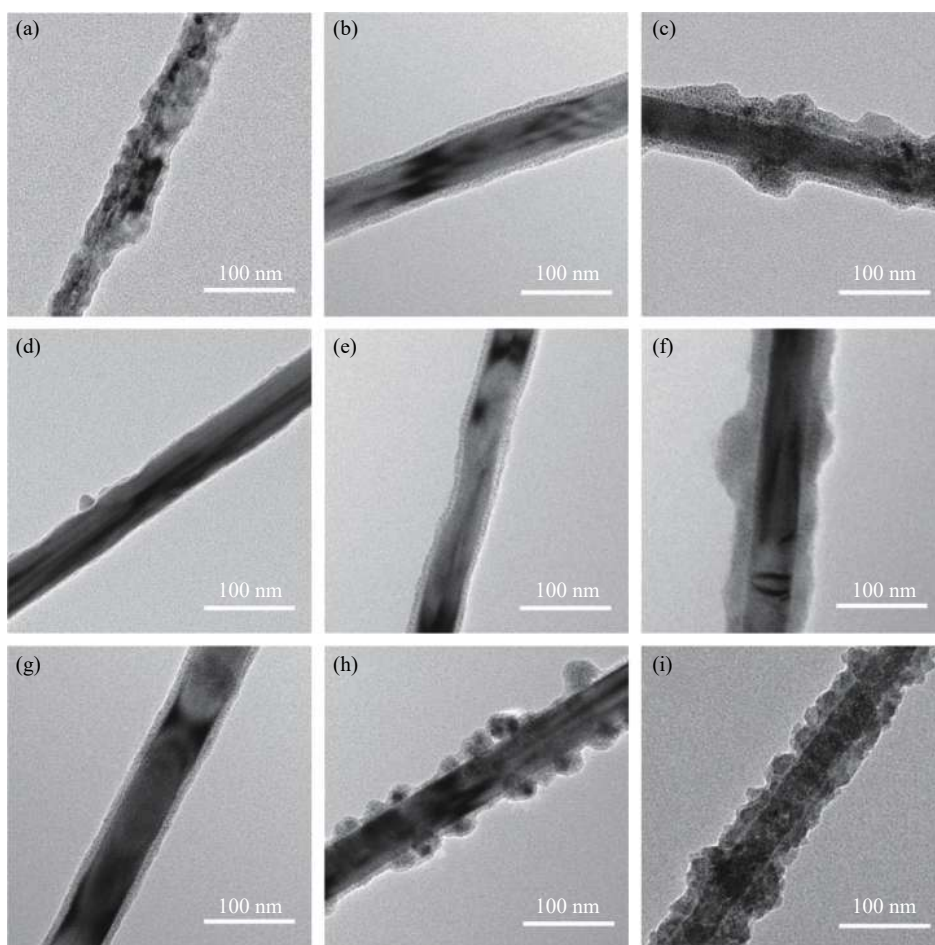


Fig. 3. TEM images of the CuNWs@C prepared with different conditions: (a)–(c) the influence of different amounts of glucose (0.5, 1.5, and 3 g in 18 mL total solution) with fixed autoclave temperature of 160°C and autoclave time of 3 h; (d)–(f) the influence of different autoclave times (1, 2, and 5 h) with fixed amount of glucose (1.5 g) and autoclave temperature of 160°C; (g)–(i) the influence of different autoclave temperatures (170, 180, and 200°C) with fixed amount of glucose (1.5 g) and autoclave time of 2 h.

perature or above, the aromatization and carbonization of the glucose could be highly accelerated and thus resulting in non-uniform film growth [22–23].

Accordingly, with an appropriate amount of glucose ($\sim 83.4 \text{ mg}\cdot\text{mL}^{-1}$) as carbon source, medium autoclave temperature of 160–170°C, and autoclave time of 2–3 h, smooth and uniform carbon layer with thickness of $\sim 8 \text{ nm}$ can be successfully *in situ* grown on CuNWs, and batch production of CuNWs@C could be realized. The uniform coating of carbon layers on different CuNWs could be directly observed by TEM as shown in Fig. 4(a). Besides, the surface morphology of the CuNWs changed strikingly after carbon coating as comparing the SEM images in Fig. 4(b) and Fig. 2(b), which further confirmed the success of our strategy in mass production of CuNWs@C. The presence of carbon element on the surface of CuNWs was further confirmed by the energy dispersive spectroscopy (EDS) (Fig. 4(c) and (d)). Notably, the oxygen observed could be due to the residual hydroxyl group on surface of the carbon layer, in agreement with the previous report [23]. The crystal structures of the CuNWs before and after carbon coating were examined by XRD and the res-

ults were presented in Fig. 4(e). The similar XRD patterns of the CuNWs and CuNWs@C indicated that there was no structure change (e.g., oxidation) occurred to CuNWs during the hydrothermal process and the carbon layers grown on CuNWs were amorphous.

As mentioned before, Cu could be easily oxidized in ambient air, especially for CuNWs with large surface area, which would significantly reduce their conductivity, presenting a big challenge for practical use of CuNWs as electrode materials. Therefore, the coating of carbon protective layer is expected to solve this problem. Fig. 4(f) compares the changes of the sheet resistances of CuNWs and CuNWs@C films upon air exposure. It can be found that the sheet resistance of bare CuNWs film increased over 150 times after 500 h exposure, while that of CuNWs@C film remained unchanged, demonstrating greatly enhanced oxidation stability of the CuNWs after carbon coating. Notably, the coating of an extra carbon layer didn't affect the conductivity of the CuNWs, due to the thin film thickness. In our preliminary study, both the bare CuNWs and CuNWs@C films could achieve less than $100 \Omega\cdot\text{sq}^{-1}$ film conductivities at average

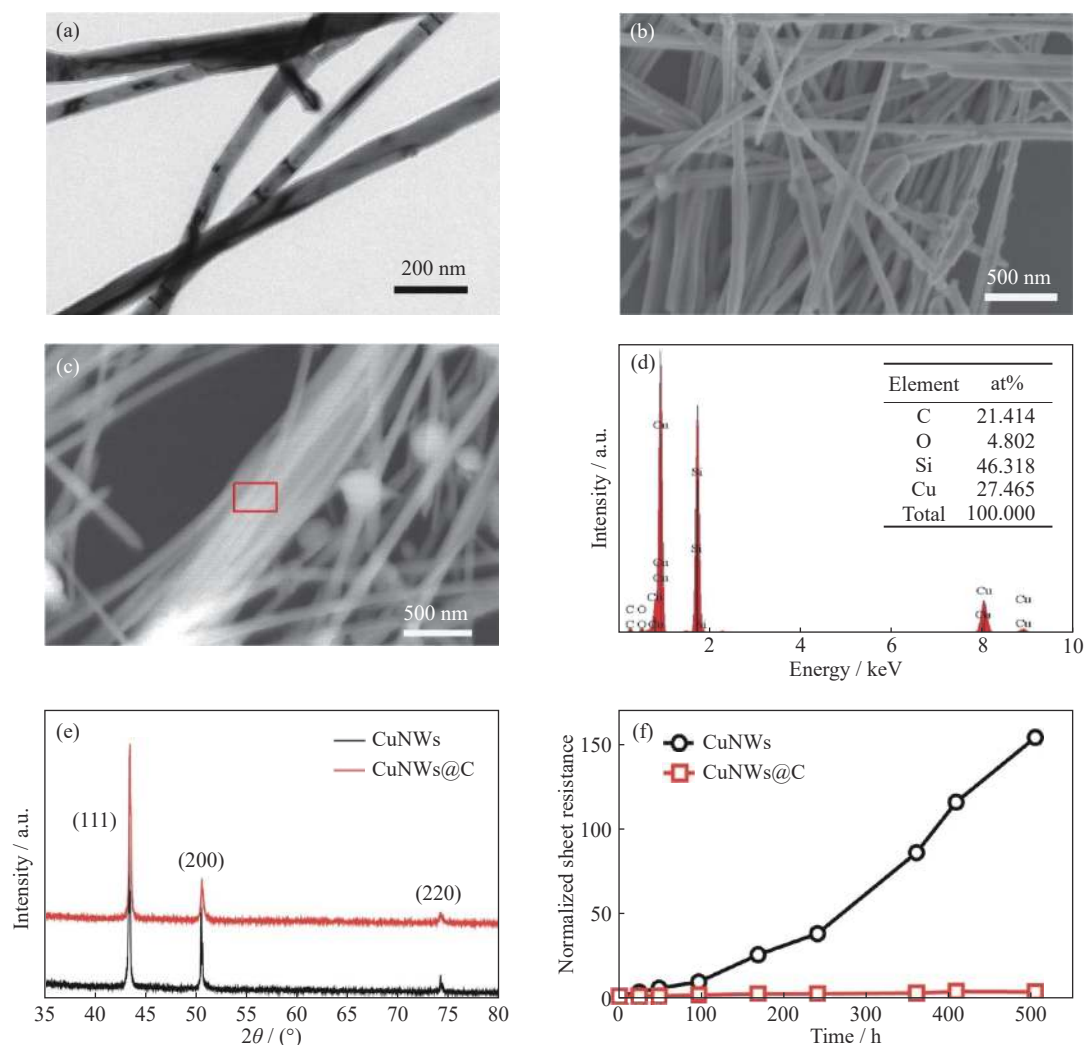


Fig. 4. (a) TEM and (b) SEM images of the CuNWs@C prepared in a batch. (c) SEM image and (d) the corresponding EDS spectrum of the CuNWs@C (on silicon substrate). (e) XRD patterns of the CuNWs and CuNWs@C. (f) Conductivity change of CuNWs and CuNWs@C films upon air exposure.

visible transmittance (AVT) around 60%–70%.

Then the chemical stability of CuNWs@C film was further evaluated by employing it as conductive substrate for preparing CE for DSSCs, where the I^-/I_3^- liquid electrolyte offers an ideal corrosive environment for stability test. Fig. 5(a) shows the device structure of the DSSC, which is composed of a dye-sensitized TiO_2 photoanode, an I^-/I_3^- electrolyte, and a CE. The CE was prepared by spin-coating of the mixed solution of polyaniline (PANI) and PEDOT:PSS on CuNWs@C conductive substrate (see details in the experimental section). In comparison, a similar CE was also prepared on bare CuNWs substrate. As can be seen in Fig. 5(b),

the CuNWs based CE resulted in quite poor photovoltaic performance with open-circuit voltage (V_{oc}) of 0.49 V, short-circuit current density (J_{sc}) of $6.15 \text{ mA}\cdot\text{cm}^{-2}$, fill factor (FF) of 0.25, and power conversion efficiency (PCE) of 0.75%, since it couldn't withstand the strong corrosion of the electrolyte. In striking contrast, the CuNWs@C based CE worked well and led to considerably higher V_{oc} of 0.63 V, J_{sc} of $14.5 \text{ mA}\cdot\text{cm}^{-2}$, FF of 0.667, and PCE of 6.1%. This result also highlights the promising application of CuNWs@C as electrode materials in perovskite solar cells, since the iodine induced corrosion of metal electrodes usually happens at the perovskite/electrode interfaces [29–34].

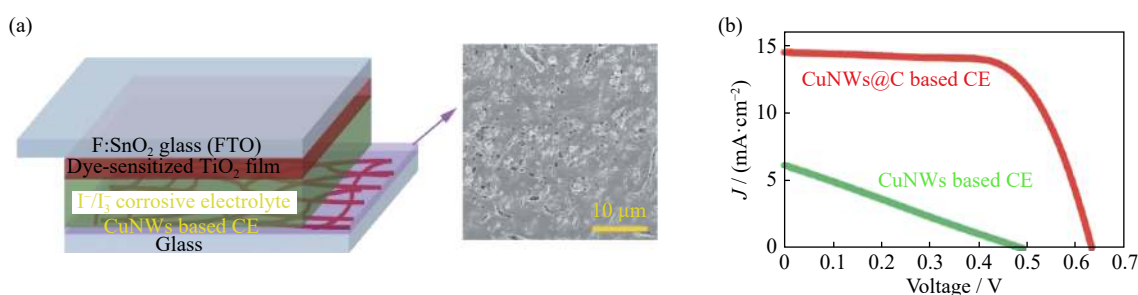


Fig. 5. (a) Device structure of DSSC and SEM image of a typical CuNWs based composite counter electrode; (b) current density (J)–voltage (V) characteristics of the DSSCs based on CEs on CuNWs and CuNWs@C substrates.

4. Conclusion

In summary, we reported a facile method for the synthesis of CuNWs@C by hydrothermal treatment of CuNWs in the presence of glucose. The influences of the amount of glucose, the hydrothermal temperature, and hydrothermal time on the growth of carbon films on CuNWs walls were systematically investigated. With glucose precursor concentration about $80 \text{ mg}\cdot\text{mL}^{-1}$, proper autoclave temperature of $160\text{--}170^\circ\text{C}$, and autoclave duration of 1–3 h, carbon layer with thickness of 3–8 nm could be uniformly grown on CuNWs, rendering greatly enhanced stability of the CuNWs@C against oxidation and chemical corrosion. Our study paves a way for the broad application of CuNWs as electrode materials for various optoelectronic devices.

Acknowledgements

This work was supported by the National Natural Science Foundation of China (No. 21403089) and the Fundamental Research Funds for the Central Universities, China (No. 2042020kf0195).

Conflict of Interest

There is no financial/commercial conflict to declare.

References

- [1] S.R. Ye, A.R. Rathmell, Z.F. Chen, I.E. Stewart, and B.J. Wiley, Metal nanowire networks: The next generation of transparent conductors, *Adv. Mater.*, 26(2014), No. 39, p. 6670.
- [2] T. Sannicolo, M. Lagrange, A. Cabos, C. Celle, J.P. Simonato, and D. Bellet, Metallic nanowire-based transparent electrodes for next generation flexible devices: A review, *Small*, 12(2016), No. 44, p. 6052.
- [3] W.T. Li, H. Zhang, S.W. Shi, J.X. Xu, X. Qin, Q.Q. He, K.C. Yang, W.B. Dai, G. Liu, Q.G. Zhou, H.Z. Yu, S.R.P. Silva, and M. Fahlman, Recent progress in silver nanowire networks for flexible organic electronics, *J. Mater. Chem. C*, 8(2020), No. 14, p. 4636.
- [4] S.A. Hashemi, S. Ramakrishna, and A.G. Aberle, Recent progress in flexible-wearable solar cells for self-powered electronic devices, *Energy Environ. Sci.*, 13(2020), No. 3, p. 685.
- [5] D.R. Wang, Y.K. Zhang, X. Lu, Z.J. Ma, C. Xie, and Z.J. Zheng, Chemical formation of soft metal electrodes for flexible and wearable electronics, *Chem. Soc. Rev.*, 47(2018), No. 12, p. 4611.
- [6] H.F. Lu, X.G. Ren, D. Ouyang, and W.C.H. Choy, Emerging novel metal electrodes for photovoltaic applications, *Small*, 14(2018), No. 14, art. No. 1703140.
- [7] A.R. Rathmell, S.M. Bergin, Y.L. Hua, Z.Y. Li, and B.J. Wiley, The growth mechanism of copper nanowires and their properties in flexible, transparent conducting films, *Adv. Mater.*, 22(2010), No. 32, p. 3558.
- [8] E.Y. Ye, S.Y. Zhang, S.H. Liu, and M.Y. Han, Disproportionation for growing copper nanowires and their controlled self-assembly facilitated by ligand exchange, *Chem. A Eur. J.*, 17(2011), No. 11, p. 3074.
- [9] A.R. Rathmell and B.J. Wiley, The synthesis and coating of long, thin copper nanowires to make flexible, transparent conducting films on plastic substrates, *Adv. Mater.*, 23(2011), No. 41, p. 4798.
- [10] M.S. Jin, G.N. He, H. Zhang, J. Zeng, Z.X. Xie, and Y.N. Xia, Shape-controlled synthesis of copper nanocrystals in an aqueous solution with glucose as a reducing agent and hexadecylamine as a capping agent, *Angew. Chem. Int. Ed.*, 50(2011), No. 45, p. 10560.
- [11] D.Q. Zhang, R.R. Wang, M.C. Wen, D. Weng, X. Cui, J. Sun, H.X. Li, and Y.F. Lu, Synthesis of ultralong copper nanowires

- for high-performance transparent electrodes, *J. Am. Chem. Soc.*, 134(2012), No. 35, p. 14283.
- [12] Y. Cheng, S.L. Wang, R.R. Wang, J. Sun, and L. Gao, Copper nanowire based transparent conductive films with high stability and superior stretchability, *J. Mater. Chem. C*, 2(2014), No. 27, p. 5309.
- [13] H. Hwang, A. Kim, Z.Y. Zhong, H.C. Kwon, S. Jeong, and J. Moon, Reducible-shell-derived pure-copper-nanowire network and its application to transparent conducting electrodes, *Adv. Funct. Mater.*, 26(2016), No. 36, p. 6545.
- [14] Z.X. Yin, S.K. Song, S. Cho, D.J. You, J. Yoo, S.T. Chang, and Y.S. Kim, Curved copper nanowires-based robust flexible transparent electrodes via all-solution approach, *Nano Res.*, 10(2017), No. 9, p. 3077.
- [15] L.T. Dou, F. Cui, Y. Yu, G. Khanarian, S.W. Eaton, Q. Yang, J. Resasco, C. Schildknecht, K. Schierle-Armdt, and P.D. Yang, Solution-processed copper/reduced-graphene-oxide core/shell nanowire transparent conductors, *ACS Nano*, 10(2016), No. 2, p. 2600.
- [16] Y. Ahn, Y. Jeong, D. Lee, and Y. Lee, Copper nanowire-graphene core-shell nanostructure for highly stable transparent conducting electrodes, *ACS Nano*, 9(2015), No. 3, p. 3125.
- [17] J.Y. Chen, W.X. Zhou, J. Chen, Y. Fan, Z.Q. Zhang, Z.D. Huang, X.M. Feng, B.X. Mi, Y.W. Ma, and W. Huang, Solution-processed copper nanowire flexible transparent electrodes with PEDOT:PSS as binder, protector and oxide-layer scavenger for polymer solar cells, *Nano Res.*, 8(2015), No. 3, p. 1017.
- [18] Y. Won, A. Kim, D. Lee, W. Yang, K. Woo, S. Jeong, and J. Moon, Annealing-free fabrication of highly oxidation-resistive copper nanowire composite conductors for photovoltaics, *NPG Asia Mater.*, 6(2014), No. 6, art. No. e105.
- [19] I.N. Kholmanov, S.H. Domingues, H. Chou, X.H. Wang, C. Tan, J.Y. Kim, H.F. Li, R. Piner, A.J.G. Zarbin, and R.S. Ruoff, Reduced graphene oxide/copper nanowire hybrid films as high-performance transparent electrodes, *ACS Nano*, 7(2013), No. 2, p. 1811.
- [20] P.C. Hsu, H. Wu, T.J. Carney, M.T. McDowell, Y. Yang, E.C. Garnett, M. Li, L. Hu, and Y. Cui, Passivation coating on electrospun copper nanofibers for stable transparent electrodes, *ACS Nano*, 6(2012), No. 6, p. 5150.
- [21] I.E. Stewart, A.R. Rathmell, L. Yan, S.R. Ye, P.F. Flowers, W. You, and B.J. Wiley, Solution-processed copper-nickel nanowire anodes for organic solar cells, *Nanoscale*, 6(2014), No. 11, p. 5980.
- [22] M.M. Titirici and M. Antonietti, Chemistry and materials options of sustainable carbon materials made by hydrothermal carbonization, *Chem. Soc. Rev.*, 39(2010), No. 1, p. 103.
- [23] X.M. Sun and Y.D. Li, Colloidal carbon spheres and their core/shell structures with noble-metal nanoparticles, *Angew. Chem. Int. Ed.*, 43(2004), No. 5, p. 597.
- [24] M. Noh, Y. Kwon, H. Lee, J. Cho, Y. Kim, and M.G. Kim, Amorphous carbon-coated tin anode material for lithium secondary battery, *Chem. Mater.*, 17(2005), No. 8, p. 1926.
- [25] E.K. Athanassiou, R.N. Grass, and W.J. Stark, Large-scale production of carbon-coated copper nanoparticles for sensor applications, *Nanotechnology*, 17(2006), No. 6, p. 1668.
- [26] X.W. Lou, J.S. Chen, P. Chen, and L.A. Archer, One-pot synthesis of carbon-coated SnO₂ nanocolloids with improved reversible lithium storage properties, *Chem. Mater.*, 21(2009), No. 13, p. 2868.
- [27] Q.D. Tai, B.L. Chen, F. Guo, S. Xu, H. Hu, B. Sebo, and X.Z. Zhao, *In situ* prepared transparent polyaniline electrode and its application in bifacial dye-sensitized solar cells, *ACS Nano*, 5(2011), No. 5, p. 3795.
- [28] Q.D. Tai, C.H. Bu, B.L. Chen, N.G. Zhang, S.H. Bai, H. Hu, S. Xu, and X.Z. Zhao, A methylene bridged bisimidazolium iodide based low-volatility electrolyte for efficient dye-sensitized solar cells, *J. Renewable Sustainable Energy*, 5(2013), No. 4, art. No. 043121.
- [29] Q.D. Tai, X.Y. Guo, G.Q. Tang, P. You, T.W. Ng, D. Shen, J.P. Cao, C.K. Liu, N.X. Wang, Y. Zhu, C.S. Lee, and F. Yan, Antioxidant grain passivation for air-stable tin-based perovskite solar cells, *Angew. Chem. Int. Ed.*, 58(2019), No. 3, p. 806.
- [30] J. Ahn, H. Hwang, S. Jeong, and J. Moon, Metal-nanowire-electrode-based perovskite solar cells: Challenging issues and new opportunities, *Adv. Energy Mater.*, 7(2017), No. 15, art. No. 1602751.
- [31] H.Y. Zhang, R. Li, W.W. Liu, M. Zhang, and M. Guo, Research progress in lead-less or lead-free three-dimensional perovskite absorber materials for solar cells, *Int. J. Miner. Metall. Mater.*, 26(2019), No. 4, p. 387.
- [32] T. Yang, Y.P. Zheng, K.C. Chou, and X.M. Hou, Tunable fabrication of single-crystalline CsPbI₃ nanobelts and their application as photodetectors, *Int. J. Miner. Metall. Mater.*, 28(2021), No. 6, p. 1030.
- [33] Y. Kato, L.K. Ono, M.V. Lee, S.H. Wang, S.R. Raga, and Y.B. Qi, Silver iodide formation in methyl ammonium lead iodide perovskite solar cells with silver top electrodes, *Adv. Mater. Interfaces*, 2(2015), No. 13, art. No. 1500195.
- [34] X.D. Li, S. Fu, W.X. Zhang, S.Z. Ke, W.J. Song, and J.F. Fang, Chemical anti-corrosion strategy for stable inverted perovskite solar cells, *Sci. Adv.*, 6(2020), No. 51, art. No. eabd1580.